Electrochemical and Solid-State Letters, **8** (7) A357-A360 (2005)
1099-0062/2005/8(7)/A357/4/$7.00 © The Electrochemical Society, Inc.

Double-Layer Capacitance of Carbide Derived Carbons in Sulfuric Acid

J. Chmiola,[a] G. Yushin,[a] R. K. Dash,[a] E. N. Hoffman,[a] J. E. Fischer,[b] M. W. Barsoum,[a] and Y. Gogotsi[a,*,z]

[a]*Department of Materials Science and Engineering, Drexel University, Philadelphia, Pennsylvania 19104, USA*
[b]*Department of Materials Science and Engineering, University of Pennsylvania, Philadelphia, Pennsylvania 19104, USA*

Nanoporous carbons obtained by selective leaching of Ti and Al from Ti_2AlC, as well as B from B_4C, were investigated as electrode materials in electric double-layer capacitors. Cyclic voltammetry tests were conducted in 1 M H_2SO_4 from 0-250 mV on carbons synthesized at 600, 800, 1000, and 1200°C. Results show that the structure and pore sizes can be tailored and that the optimal synthesis temperature is 1000°C. Specific capacitances for Ti_2AlC CDCs and B_4C CDCs were 175 and 147 F/g, respectively, compared to multiwall carbon nanotubes and two types of activated carbon, measured herein to be 15, 52, and 125 F/g, respectively.
 [DOI: 10.1149/1.1921134]

Manuscript submitted December 22, 2004; revised manuscript received February 18, 2005. Available electronically May 17, 2005.

Research interest in highly porous carbons has increased in recent years for a number of different applications such as methane and hydrogen storage, adsorbents, catalyst supports, as well as electrochemical double layer capacitors (EDLCs).[1] EDLCs use non-Faradaic charge separation across an electrolyte/electrode interface to store electrical energy. In general, an EDLC behaves like a traditional parallel plate capacitor, whereby the capacitance is roughly proportional to the surface area of the plates. The dependence of capacitance on specific surface area (SSA) is not, however, linear. Micropores (pores with diameters less than 2 nm) contribute to most of the SSA, but the smallest ones may not be accessible to the electrolyte. It is therefore important to design a carbon electrode which has pores that are large enough to be completely accessed by the electrolyte, but small enough to result in a large SSA. In general, pore sizes of roughly twice the solvated ion size should be sufficient to contribute to double-layer capacitance.[2] For an aqueous electrolyte, pores as small as 0.5 nm should be accessible. For solvated ions in aprotic media, larger pores are needed.[3] Consequently, it is important to tailor the pore size distribution in the electrode material to match that needed to maximize the specific capacitance.

Various carbonaceous materials have been studied as electrode materials for EDLCs, such as activated organic materials,[4] carbonized polymers,[5,6] aerogels,[7] carbon fibers,[8] and nanotubes.[9-12] These have different pore structures and surface chemistries due to the different processing techniques and starting materials. Kim *et al.* showed specific capacitances of 100 F/g for carbonized polymer in an aqueous electrolyte, but only 5 F/g in an organic electrolyte with larger ions.[6] The use of templating agents to produce carbons with controlled pore size distribution results in specific capacitances as high as 200 F/g when organic electrolytes are used.[13-15] This technique is limited to producing mesopores (pores with a diameter greater than 2 nm), and is not suited to scale-up due to lengthy processing. At 180 F/g,[9] modified single-wall nanotubes exhibit large specific capacitance, but their cost is prohibitive. Multi-wall carbon nanotubes, because of low specific surface area, traditionally have low specific capacitance. Etching or other post-treatments have increased the performance of these materials significantly, but activated carbons still remain superior.[16,17]

Recently, a new group of porous carbon materials, carbide derived carbons (CDCs), have been receiving attention in the literature for applications in EDLCs.[18-21] CDCs are obtained by selective leaching of metals from metal carbides with halogens.[22] The resulting carbon has high SSA, with pore sizes that can be fine-tuned by controlling the chlorination temperature and by the choice of starting carbide.[23] Our previous work showed high SSA with a narrow pore size distributions,[24,25] suggesting high specific capacitances. The present study focuses on the effect of synthesis temperature on the double layer capacitance of CDCs produced from B_4C and Ti_2AlC.

Experimental

B_4C powder (Alfa Asear, Ward Hill, MA) of 2.53 g/cm^3 density, 99.4% purity and 6 μm average particle size was chlorinated at 600, 800, 1000, and 1200°C. Bulk Ti_2AlC pieces, (3-ONE-2, Vorhees, NJ) were chlorinated at temperatures of 600, 800, and 1000°C. These samples were crushed in a mortar after chlorination to produce powder. Details of the chlorination technique have been reported previously.[22,24,25]

Porosity analysis was carried out at −195.8°C using a Quantachrome Autosorb-1 and N_2 and Ar as the adsorbates. Pore size distributions were calculated from Ar adsorption data using the density functional theory (DFT) method[26] provided by Quantachrome data reduction software version 1.27 and the SSA was calculated using the Brunauer, Emmet, Teller (BET) method.[27]

The powders were processed into capacitor electrodes by mixing them with 5 wt% Teflon (E.I. du Pont de Nemours, Wilmington, DE) powder, homogenized in a mortar and pestle, and finally rolled into a thin film of uniform thickness (~175 μm). Four-probe conductivity measurements showed the resistivity of the CDC to be on the order of 1 Ω-cm^{-1}, which was low enough to eliminate the need for carbon black additions. From this film, 1 cm^2 circular electrodes were punched out and inserted into a two electrode test cell with a porous polypropylene separator (Celgard Inc., Charlotte, NC) and a 1 M H_2SO_4 aqueous electrolyte. Electrode films were also prepared from an activated carbon with a low SSA (Alfa Asear, Ward Hill, MA) and one with a SSA comparable with our materials (Arkema, Serquigny, France), which will be referred to henceforth as advanced activated carbon, as well as multi-wall carbon nanotubes (Arkema, Serquigny, France) for comparison. CV experiments were conducted between 0 and 250 mV using a Princeton Applied Research 273 potentiostat/galvanostat. The specific capacitances were calculated from data taken at a scan rate of 1 mV/s.

Results and Discussion

The CDCs synthesized at low temperatures were amorphous. Higher temperature synthesis generally resulted in the formation of graphitic structures. Figure 1a shows a transmission electron microscopy (TEM) image of CDC produced from Ti_2AlC at 400°C. The highly disordered structure of the material is clearly seen. Ti_2AlC synthesized at 1200°C (Fig. 1b) demonstrated a network of graphitic

* Electrochemical Society Active Member.
z E-mail: Gogotsi@drexel.edu

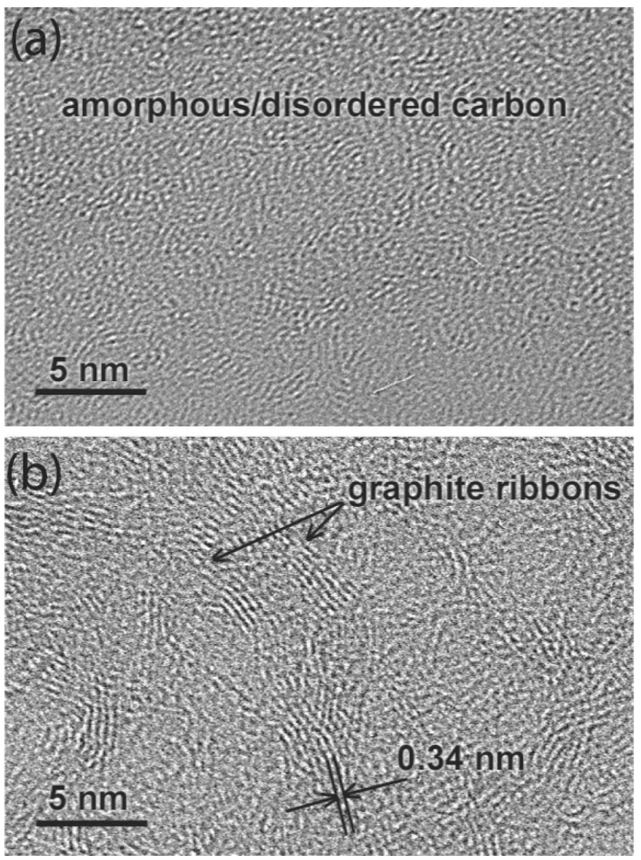

Figure 1. Representative TEM images of Ti_2AlC CDCs synthesized at temperatures of (a) 600 and (b) 1200°C. Structure of CDC samples depends on the synthesis temperature. Samples prepared at low temperatures are amorphous; those prepared at higher temperatures contained graphite ribbons.

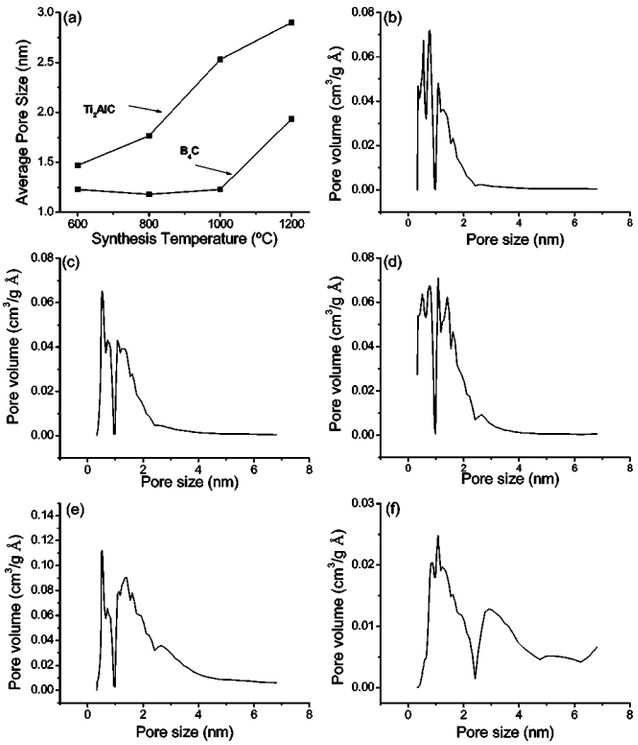

Figure 2. (a) Average pore widths calculated using Ar as the adsorbate, density functional theory and a weighted method which takes into account contributions of pore volume. (b) Pore size distribution for advanced activated carbon, B_4C CDC synthesized at (c) 600 and (d) 1000°C, and Ti_2AlC CDC synthesized at (e) 600 and (f) 1000°C.

ribbons mixed in with a more disordered carbon structure. The structure of B_4C CDC synthesized in this temperature range was similar.[25] Synthesis of CDC at a temperature of 1000°C resulted in a more graphitic structure than activated carbon, without a compromise in specific surface area.

Pore sizes for Ti_2AlC CDCs[24] and B_4C CDCs[25] calculated using DFT show that the average pore diameter increases with synthesis temperature (Fig. 2a). Although the distribution figures (Fig. 2b-f) show multi-modal pore size distributions with minima of zero, this is an artifact of the DFT model. The actual pore size distribution, though it may be multimodal, is believed to be more uniform. The advanced activated carbon PSD (Fig. 2b) exhibits a pore structure much like B_4C CDC synthesized at low temperatures, with an average pore diameter of ~1 nm and a fraction of larger pores up to ~2.5 nm. The low SSA activated carbon has an average pore size of ~0.5 nm. Figures 2c and d are representative of the changes in pore structure of B_4C CDC with synthesis temperature. At 600°C the total pore volume is comprised largely of microporosity, whereas at 1000°C the pore size distribution widens and shifts to larger average pore diameters. Ti_2AlC CDC has a more pronounced widening of the pore size distribution at higher synthesis temperatures, with the 1000°C sample having a large fraction of mesopores larger than 2 nm (Fig. 2f).

As shown herein, large SSAs can be obtained for CDCs without further activation of the carbon product (Fig. 3). In Ti_2AlC CDCs, the SSAs calculated from N_2 adsorption increase from ~800 m^2/g after chlorination at 600°C to a maximum of ~1550 m^2/g after chlorination at 1000°C (Fig. 3a). The SSA then decreases as the chlorination temperature increases most probably due to increasing graphitization and closing off of small pores of the amorphous carbon B_4C CDC has a maximum SSA of ~1800 m^2/g after chlorination at 800°C (Fig. 3b). The SSAs of both CDCs are dominated by pores that are accessible to the aqueous electrolyte ions. The SSAs of the low SSA activated carbon, advanced activated carbon and carbon nanotubes were 547, 1225, and 180 m^2/g, respectively.

CV tests were conducted to characterize electrochemical performance. No faradaic reactions were found within the voltage window of interest for either material (Fig. 4 and 5). B_4C CDC synthesized at faradaic 600°C resulted in a specific capacitance of 95 F/g, increasing to 147 F/g after 1000°C synthesis (Fig. 4a and 2b). The latter turned out to be the optimum synthesis temperature; at 1200°C the value dropped to 120 F/g. This trend follows that of the BET SSA. The observed small deviations may be connected to the incomplete accessibility of the smallest pores to the electrolyte ions. Ti_2AlC CDC's followed even closer the correlation between capacitance and SSA (Fig. 4b and 3a): synthesis at 600°C resulted in a specific capacitance of 77 F/g, while at 1000°C it was 175 F/g, the highest of all materials tested. For comparison, low SSA activated carbon, advanced activated carbon and carbon nanotubes yielded 52, 125, and 15 F/g, respectively. The low specific capacitance value for the low SSA activated carbon and nanotube samples correlate with their low SSAs, ~550 and ~180 m^2/g, respectively.

When normalized by their SSAs, CDC capacitors still had higher specific capacitance than the MWNTs tested: 8.7 $\mu F/cm^2$ for B_4C CDC synthesized at 1000°C, 11.3 $\mu F/cm^2$ for Ti_2AlC CDC synthesized at 1000°C, 8 $\mu F/cm^2$ for MWNTs, 10 $\mu F/cm^2$ for advanced activated carbon, and 9.5 $\mu F/cm^2$ for the low SSA activated carbon sample. Localized oxygen containing functional groups generated during the carbon activation contribute to higher surface reactivity and may explain the larger specific capacitance compared to B_4C CDC.[1] The influence of oxygen-containing functional groups in ac-

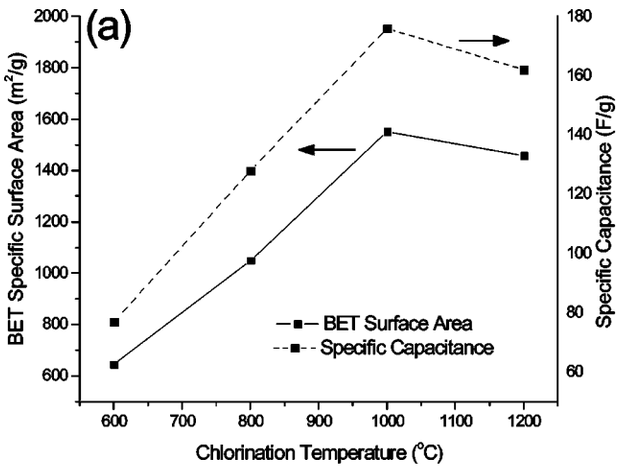

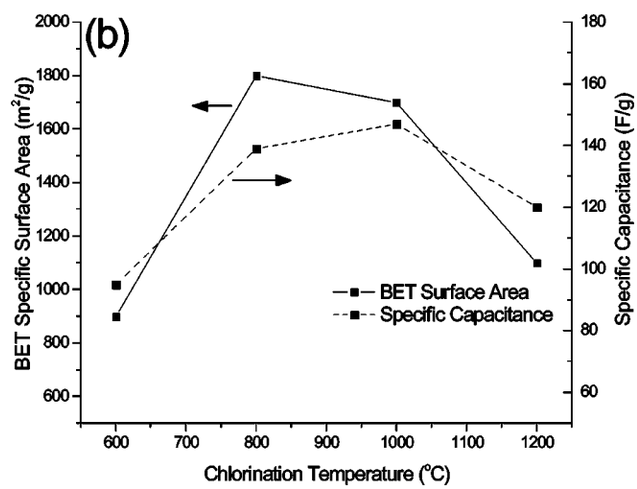

Figure 3. BET SSA and specific capacitance vs. chlorination temperature for (a) Ti_2AlC CDC and (b) B_4C CDC. The linear correlation between these parameters for Ti_2AlC CDCs suggests that most of the CDC pores are accessible to the electrolyte ions, irrespective of the synthesis temperature. The small deviations from the linear dependence of the specific capacitance and the SSA seen in B_4C CDCs may be due to the incomplete accessibility of the smallest pores to the electrolyte.

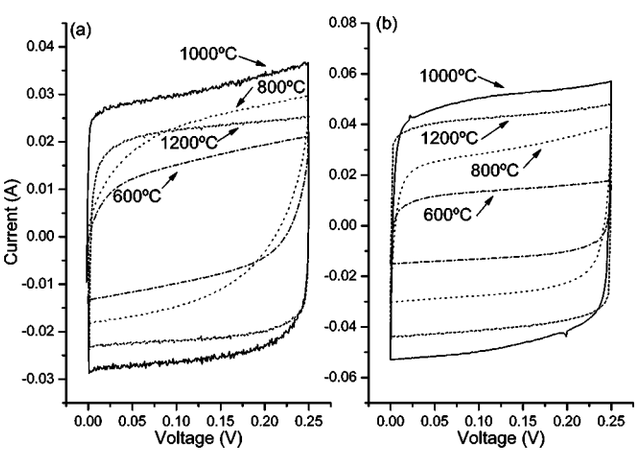

Figure 4. CVs obtained from tests run at a scan rate of 1 mV/s on (a) B_4C CDCs and (b) Ti_2AlC CDCs.

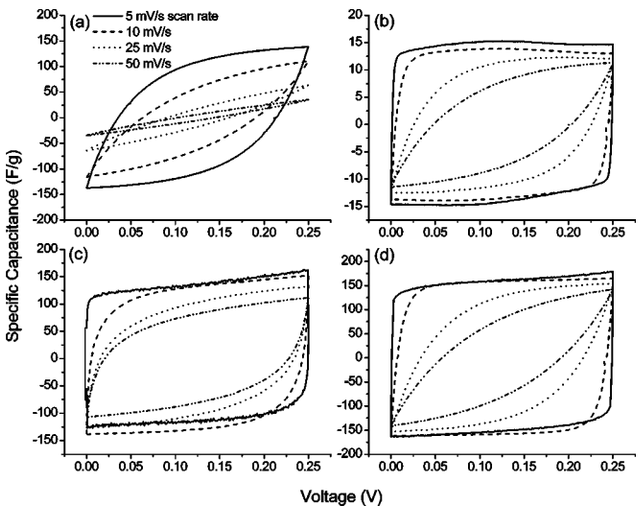

Figure 5. CVs taken at scan rates of 5, 10, 25, and 50 mV/s for (a) advanced activated carbon, (b) multi-wall carbon nanotubes, (c) B_4C CDC synthesized at 1000°C and (d) Ti_2AlC CDC synthesized at 1000°C. Activated carbon with the smallest pores showed the slowest current response at high scan rates.

tivated carbon is not enough to generate specific capacitances greater than the highly developed porous structure in Ti_2AlC, however.

CV tests from 5 to 50 mV/s and $0 < V < 250$ mV were performed to gain a qualitative understanding of the influence of pore structure on the rate dependence of the charge-discharge behavior. Deviations from ideal behavior are found at the highest scan rates (Fig. 5), where the current response is slower in more microporous electrodes. Ti_2AlC CDC and B_4C CDC synthesized at 1000°C have the largest fraction of mesopores (>2 nm width) and show only small deviations from ideal behavior at 50 mV/s (Fig. 5c). Advanced activated carbon has the smallest pores and shows the poorest high-rate performance. Further optimization of the porous structure of CDCs should yield even better specific capacitances and lower rate constants.

Conclusions

Porous carbon electrodes were produced by selective leaching of titanium and aluminum from titanium aluminum carbide and boron from boron carbide. The resulting CDC electrodes exhibited specific capacitances that depended on the pore size and SSA, both of which can be controlled by the synthesis temperature. Ti_2AlC CDCs and B_4C CDCs, produced at a temperature of 1000°C, showed maximum specific capacitances of 175 and 147 F/g, respectively. These values are comparable to the best carbon materials reported in literature for use in EDLCs. At temperatures above and below 1000°C, the specific capacitances decrease as a result of decreasing SSAs. Our ability to control the porous structure of the carbon electrodes means that further tuning of the CDC structure should result in even higher specific capacitance. Activated carbons and multiwall carbon nanotubes prepared and tested under the same conditions as CDCs had specific capacitances of 52, 125, and 15 F/g, respectively, all values lower than the best performing CDCs synthesized herein. CDC synthesized at 1000°C had good performance in cyclic voltammetry up to a scan rate of at least 50 mV/s.

Acknowledgments

This work was supported by Arkema, France. We are grateful to Dr. T. El-Raghy of 3-ONE-2, Vorhees, NJ, for supplying us the Ti_2AlC samples used in this work and many fruitful discussions. Some of the authors were supported by the U.S. Department of Energy, DE-FG02-98ER45701 and by DARPA via ONR contract.

E.H. was supported by NSF IGERT Fellowship and DMR 0072067. HRTEM was performed in the Penn Regional Nanotechnology Facility at the University of Pennsylvania.

Drexel University assisted in meeting the publication costs of this article.

References

1. B. E. Conway, *Electrochemical Capacitors: Scientific Fundamentals and Technological Applications*, Kluwer, New York (1999).
2. M. Endo, T. Maeda, T. Takeda, Y. J. Kim, K. Koshiba, H. Hara, and M. S. Dresselhaus, *J. Electrochem. Soc.*, **148**, A910 (2001).
3. F. Beguin, *Carbon*, **39**, 937 (2001).
4. Y. Guo, J. Qi, Y. Jiang, S. Yang, Z. Wang, and H. Xu, *Mater. Chem. Phys.*, **80**, 704 (2003).
5. M. Endo, Y. J. Kim, K. Osawa, K. Ishii, T. Inoue, T. Nomura, N. Miyashita, and M. S. Dresselhaus, *Electrochem. Solid-State Lett.*, **6**, A23 (2003).
6. Y. J. Kim, Y. Masutzawa, S. Ozaki, M. Endo, and M. S. Dresselhaus, *J. Electrochem. Soc.*, **151**, E199 (2004).
7. R. Saliger, U. Fischer, C. Herta, and J. Fricke, *J. Non-Cryst. Solids*, **225**, 81 (1998).
8. H. Nakagawa, A. Shudo, and K. Miura, *J. Electrochem. Soc.*, **147**, 38 (2000).
9. E. Frackowiak, K. Jurewicz, S. Depleux, and F. Beguin, *J. Power Sources*, **97-98**, 822 (2001).
10. K. H. An, K. K. Jeon, J. K. Heo, S. C. Lim, D. J. Bae, and Y. H. Lee, *J. Electrochem. Soc.*, **149**, A1058 (2002).
11. F. Pico, J. M. Rojo, M. L. Sanjuan, A. Anson, A. M. Benito, M. A. Callejas, W. K. Maser, and M. T. Martinez, *J. Electrochem. Soc.*, **151**, A831 (2004).
12. Y. k. Zhou, B. l. He, W. j. Zhou, and H. l. Li, *J. Electrochem. Soc.*, **151**, A1052 (2004).
13. S. Yoon, Y. Lee, T. Hyeon, and S. M. Oh, *J. Electrochem. Soc.*, **147**, 2501 (2000).
14. T. Hisashi, K. Masayuki, M. Masayuki, and Y. Hajime, *Electrochem. Solid-State Lett.*, **6**, A214 (2003).
15. H. Zhou, S. Zhu, M. Hibino, and I. Honma, *J. Power Sources*, **122**, 219 (2003).
16. E. Frackowiak, S. Delpeux, K. Jurewicz, K. Szostak, D. Cazorla-Amoros, and F. Beguin, *Chem. Phys. Lett.*, **361**, 35 (2002).
17. Q. Xiao and X. Zhou, *Electrochim. Acta*, **48**, 575 (2003).
18. R. G. Avarbz, A. V. Vartanova, S. K. Gordeev, S. G. Zjukov, B. A. Zelenov, A. E. Kravtjik, V. P. Kuznetsof, J. A. Kukusjkina, T. V. Mazaeva, O. S. Pankina, and V. V. Sokolov, U.S. Pat. 6,110,335 (1998).
19. A. Burke, *J. Power Sources*, **91**, 37 (2000).
20. Y. A. Malentin, N. G. Strizhakova, V. Y. Izotov, A. A. Mironova, S. G. Kozachkov, V. A. Danilin, S. N. Podmogilny, M. Arulepp, K. J. Aleksandrovna, K. A. Efimovitj, S. V. Vasilevitj, A. Perkson, J. Leis, J. Zheng, G. S. Konstantinovich, J. Y. Kolotilova, J. Cederstrom, and C. L. Wallace, WO 02/39468 A2, 2002.
21. E. Lust, A. Janes, and M. Arulepp, *J. Electroanal. Chem.*, **562**, 33 (2003).
22. A. Nikitin and Y. Gogotsi, in *Encyclopedia of Nanoscience and Nanotechnology*, Vol. 7, H. S. Nalwa, p. 553, American Scientific Publishers, Stevenson Ranch, CA (2003).
23. Y. Gogotsi, A. Nikitin, H. Ye, W. Zhou, J. E. Fischer, B. Yi, H. C. Foley, and M. W. Barsoum, *Nat. Mater.*, **2**, 591 (2003).
24. E. N. Hoffman, G. Yushin, M. W. Barsoum, and Y. Gogotsi, *Chem. Mater.*, Submitted.
25. R. K. Dash, A. Nikitin, and Y. Gogotsi, *Microporous Mesoporous Mater.*, **72**, 203 (2004).
26. N. A. Seaton, J. P. R. B. Walton, and N. Quirke, *Carbon*, **27**, 853 (1989).
27. S. Brunauer, P. H. Emmett, and E. Teller, *J. Am. Ceram. Soc.*, **60**, 309 (1938).